Reactivity of O_2 versus H_2O_2 with polysaccharide monooxygenases

John A. Hangasky[a], Anthony T. Iavarone[a,b], and Michael A. Marletta[a,b,c,1]

[a]California Institute for Quantitative Biosciences, University of California, Berkeley, CA 94720; [b]Department of Chemistry, University of California, Berkeley, CA 94720; and [c]Department of Molecular and Cell Biology, University of California, Berkeley, CA 94720

Contributed by Michael A. Marletta, March 28, 2018 (sent for review January 22, 2018; reviewed by Kenneth D. Karlin and JoAnne Stubbe)

Enzymatic conversion of polysaccharides into lower-molecular-weight, soluble oligosaccharides is dependent on the action of hydrolytic and oxidative enzymes. Polysaccharide monooxygenases (PMOs) use an oxidative mechanism to break the glycosidic bond of polymeric carbohydrates, thereby disrupting the crystalline packing and creating new chain ends for hydrolases to depolymerize and degrade recalcitrant polysaccharides. PMOs contain a mononuclear Cu(II) center that is directly involved in C–H bond hydroxylation. Molecular oxygen was the accepted cosubstrate utilized by this family of enzymes until a recent report indicated reactivity was dependent on H_2O_2. Reported here is a detailed analysis of PMO reactivity with H_2O_2 and O_2, in conjunction with high-resolution MS measurements. The cosubstrate utilized by the enzyme is dependent on the assay conditions. PMOs will directly reduce O_2 in the coupled hydroxylation of substrate (monooxygenase activity) and will also utilize H_2O_2 (peroxygenase activity) produced from the uncoupled reduction of O_2. Both cosubstrates require Cu reduction to Cu(I), but the reaction with H_2O_2 leads to nonspecific oxidation of the polysaccharide that is consistent with the generation of a hydroxyl radical-based mechanism in Fenton-like chemistry, while the O_2 reaction leads to regioselective substrate oxidation using an enzyme-bound Cu/O_2 reactive intermediate. Moreover, H_2O_2 does not influence the ability of secretome from *Neurospora crassa* to degrade Avicel, providing evidence that molecular oxygen is a physiologically relevant cosubstrate for PMOs.

oxygen | hydrogen peroxide | monooxygenase

The utilization of molecular oxygen (O_2) is essential for numerous biological processes. Although a powerful oxidant, biological utilization involves reduction at metal centers such as iron and copper to generate oxidants capable of a wide range of reactions with organic molecules. Oxygenases have evolved to generate a reactive O_2 species capable of selective O-atom insertion into an unactivated C–H bond while controlling aberrant side reactions and the leakage of reactive oxidant species into solution (1). Cu-dependent polysaccharide monooxygenases (PMOs), also known as lytic PMOs, are found in eukaryotic and prokaryotic organisms (2) and are secreted into the extracellular environment to degrade polysaccharides through an oxidative mechanism. Over the past decade, research on this enzyme family has intensified as PMOs have emerged as potential catalysts in biofuel production (3, 4) and have been implicated in various physiological processes (5, 6).

Recently H_2O_2, rather than O_2, was reported to be the physiological cosubstrate utilized by PMOs (7). While the peroxygenase activity of PMOs may have implications in industrial applications, such activity in a biological setting would be distinct from that of known peroxygenases, which employ a ferric heme cofactor that can stabilize reactive intermediates similar to P450s (8, 9). In the presence of a reductant, but in the absence of a polysaccharide substrate, PMOs reduce O_2 (10) and generate H_2O_2 (11). O_2 reduction in the presence of a polysaccharide substrate is expected to lead to substrate oxidation, similar to other well-characterized O_2-activating Cu enzymes (12).

The heterogeneity of reactions with large, insoluble polysaccharide substrates hinders substrate loading of the PMO and complicates biochemical studies, especially when the substrate-free enzyme leads to the uncoupling of O_2 activation (reduction) from substrate oxidation. Under these reaction conditions it can be difficult to distinguish oxygenase activity from peroxygenase activity resulting from the in situ generation of H_2O_2 (Fig. 1*A*). The ability of some PMOs to oxidize soluble oligosaccharides allows for homogenous reaction mixtures that overcome the concentration ambiguity of insoluble substrates, as well as suppressing the uncoupled reaction (11, 13, 14). Recently reported crystal structures of oligosaccharide-bound PMOs have provided insight to the active-site environment and the positioning of the polysaccharide substrate in C4-oxidizing PMOs (15). The glycosidic bond connecting the second and third glycosyl units (from the reducing end) is positioned over the Cu active site, such that regioselective oxidation would generate Glc2ox [β-D-xylo-hexos-4-ulopyranosyl-(1 → 4)-β-D-glucopyranosyl], which would subsequently hydrate in a nonenzymatic chemical step to form a geminal diol [Glc2gem, 4-hydroxy-β-D-xylo-hexopyranosyl-(1 → 4)-β-D-glucopyranosyl] as the only products (Fig. 1*B*).

In this paper, we investigated the cosubstrate dependence on the oxidative degradation of three cellulosic substrates by *Mt*PMO9E, a C4-oxidizing PMO from *Thermothelomyces thermophila* (formerly *Myceliophthora thermophila*). The cosubstrate (O_2 or H_2O_2) utilized by the PMO to oxidize the polysaccharide was dependent on the substrate concentration, as well as the solubility of the cellulosic substrate. Based on these findings, MS was used to compare the product profiles and modifications of the PMO resulting from the reaction with either cosubstrate in the presence and absence of the soluble substrate cellohexaose. Results indicated differences in PMO modification, as well as the product

Significance

Since the discovery of polysaccharide monooxygenases (PMOs), attention has focused on structure, function, and mechanism. The PMO copper active site can utilize oxygen or hydrogen peroxide to catalyze substrate oxidation. Although oxygen has been considered to be the physiologically relevant cosubstrate in the reaction, recent reports have focused on hydrogen peroxide. While oxygen is acknowledged as the cosubstrate utilized for other biological copper-dependent hydroxylations, there is no reason to rule out hydrogen peroxide for PMOs. This paper provides a detailed kinetic analysis and characterization of PMO reactivity with each cosubstrate. PMOs are capable of using either cosubstrate to oxidize the glycosidic linkage of cellulosic substrates, but different molecular mechanisms are accessed that affect enzyme activity and the products formed.

Author contributions: J.A.H. and M.A.M. designed research; J.A.H. and A.T.I. performed research; J.A.H., A.T.I., and M.A.M. analyzed data; M.A.M. performed overall supervision; and J.A.H., A.T.I., and M.A.M. wrote the paper.

Reviewers: K.D.K., Johns Hopkins University; and J.S., Massachusetts Institute of Technology.

The authors declare no conflict of interest.

[1]To whom correspondence should be addressed. Email: marletta@berkeley.edu.

This article contains supporting information online at www.pnas.org/lookup/suppl/doi:10.1073/pnas.1801153115/-/DCSupplemental.

Published online April 23, 2018.

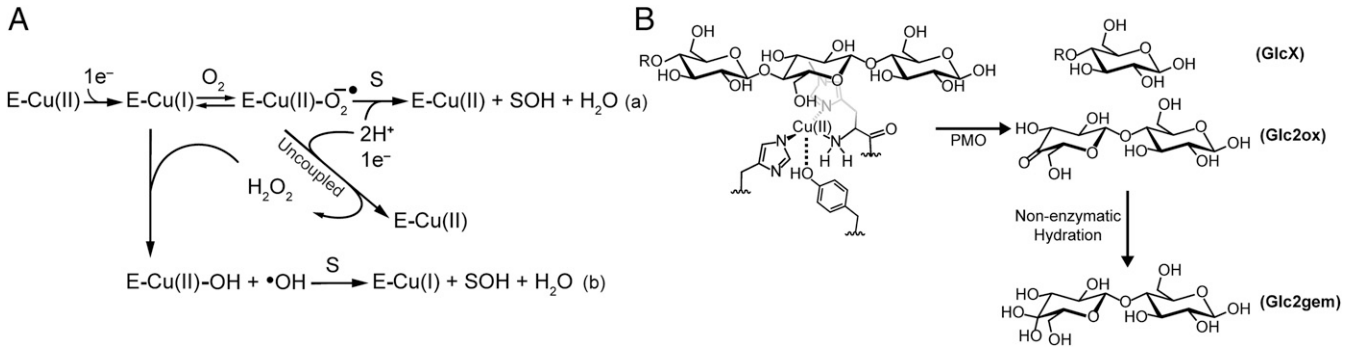

Fig. 1. Minimal reaction schemes for PMOs. (*A*) O_2 binds to the Cu(I) active site. In the presence of a polysaccharide substrate, O_2 reduction leads to substrate hydroxylation (pathway a). In the absence of a polysaccharide substrate, O_2 reduction produces H_2O_2. In situ-generated H_2O_2 can rereact with the Cu(I) active site. When the polysaccharide substrate is bound, substrate oxidation will occur (pathway b). E, PMO; S, polysaccharide substrate. (*B*) Substrate positioning favors C4-oxidation of the second glucosyl group. Nonenzymatic hydration of 4-ketoaldose product forms a geminal diol (Glc2gem). Either small-molecule reductants or CDH can provide the necessary reducing equivalents for this transformation. Active-site homology model based on Protein Data Bank ID code 5ACF (15). GlcX, cello-oligosaccharide with degree of polymerization = X; R, additional glycosyl unit(s).

distribution resulting from an equal number of turnovers of oxidant. In addition, kinetic analysis of O_2- and H_2O_2-dependent reactivity provides a rationale for the catalytic properties associated with peroxygenase and oxygenase activity. The results presented herein support O_2 as a cosubstrate for PMOs to oxidize polysaccharide substrates, as originally proposed for this family of enzymes (16, 17), and draw sharp distinctions from the reaction with H_2O_2.

Results

Comparison of Oxidative Activity on Cellulosic Substrates. Avicel (microcrystalline cellulose), phosphoric acid swollen cellulose (PASC), and cellohexaose (Glc6) vary in their physical properties including crystallinity, microfibril shape, specific surface area, and average degree of polymerization. These properties directly affect polysaccharide solubility and the concentration of PMO-accessible chains (18, 19). The PMO *Mt*PMO9E was chosen to directly compare activity on these three cellulosic substrates. *Mt*PMO9E regiospecifically hydroxylates the C4 position of cellulose as well as soluble cellodextrins (*SI Appendix*, Figs. S1–S5 and Tables S1–S6) and as such serves as a good PMO model with reaction specificity. The uncoupled *Mt*PMO9E reaction results in the formation of H_2O_2 (Fig. 2*A*), which is

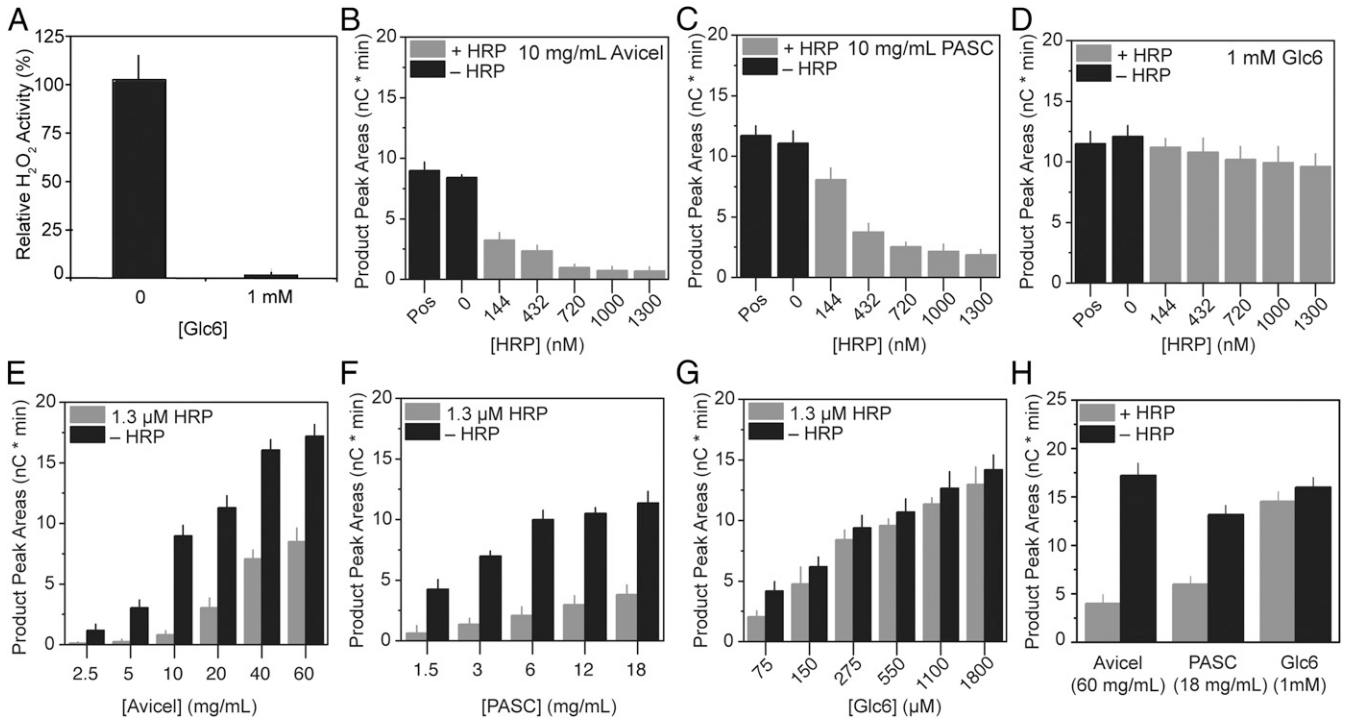

Fig. 2. *Mt*PMO9E activity on cellulosic substrates in the presence of HRP. *A* shows the suppression of H_2O_2 formation by Glc6 (1 mM). Assays contained HRP (1 μM), Amplex Red (200 μM), *Mt*PMO9E (1 μM), ascorbic acid (50 μM), and cellohexaose (0 or 1 mM) (n = 5). Assays for *B*–*D* contained *Mt*PMO9E (1 μM), ascorbate (2 mM), cellulosic substrate (Avicel, PASC, or Glc6), Amplex Red (200 μM), and HRP (0–1.3 μM) (n = 3). Pos, control assay containing all reaction components except Amplex Red. Assay for *E*–*G* contained *Mt*PMO9E (1 μM), ascorbate (2 mM), cellulosic substrate (Avicel, PASC, or Glc6), Amplex Red (200 μM), and HRP (0 or 1.3 μM) (n = 3). Assays in *H* contained *Mt*PMO9E (1 μM), *Mt*CDH2 (1 μM), Glc2 (2 mM), cellulosic substrate (Avicel, PASC, or Glc6), Amplex Red (200 μM), and HRP (0 or 1.3 μM) (n = 3). All assays were performed in 50 mM MES [2-(*N*-morpholino)ethanesulfonic acid] and 50 mM MOPS (3-morpholinopropane-1-sulfonic acid), I = 100 mM, pH 6.5 at 40 °C. Error bars represent one SD of the mean.

known to participate in the oxidation of polysaccharides (7). *Mt*PMO9E activity on the three cellulosic substrates was tested in the presence of increasing concentrations of HRP to distinguish O_2-dependent oxidations from H_2O_2-dependent oxidations. Subsequent assays used increasing substrate concentrations in the presence of an excess concentration of HRP (1.3 μM) relative to the PMO (1 μM) to maximize substrate loading of the enzyme. It is important to note that only the soluble products released from Avicel and PASC oxidation were monitored.

The total soluble oxidized products resulting from the reaction with the two insoluble substrates, Avicel and PASC, were significantly influenced by the concentration of HRP in the assay (Fig. 2 *B* and *C*). Excess HRP relative to the PMO essentially inhibited the generation of oxidized products from Avicel (8 ± 4%) and only had a slightly less inhibitory effect with PASC (15 ± 3%). When the concentration of Avicel or PASC was increased, less inhibition by excess HRP was observed (Fig. 2 *E* and *F*).

The primary reaction with homogenous reaction mixtures containing the soluble substrate Glc6 is the coupled reaction of O_2 reduction and substrate hydroxylation (Fig. 2*D*). A correlation between substrate concentration and the total oxidized products was observed when an excess concentration of HRP was used in the reaction mixtures. Subsaturating Glc6 concentrations (i.e., [Glc6] < $K_{m(Glc6)}$, discussed below) resulted in a nearly 50% decrease in reaction products, whereas HRP had less of an inhibitory effect with increasing Glc6 concentrations (Fig. 2*G*). At Glc6 concentrations greater than 275 μM, the total oxidized products decreased by less than 10%. In addition to a nominal effect on activity by HRP, H_2O_2 was not detected in the presence of high concentrations of Glc6 (Fig. 1*A*) and yet O_2 consumption was observed (*SI Appendix*, Fig. S6).

Cellobiose dehydrogenase (CDH) reduces PMOs directly (20, 21) and reduces O_2 slowly (22), which will limit the in situ generation of H_2O_2. Therefore, the above assays were repeated substituting ascorbic acid with CDH (1 μM) from *T. thermophila* (*Mt*CDH2) and the CDH substrate cellobiose (Glc2) (2 mM). The addition of HRP to the reaction mixtures containing either Avicel or PASC led to 75% and 56% reduction in soluble oxidized products, respectively, indicating that the *Mt*CDH2-dependent PMO activity was equally uncoupled compared with the reactions with ascorbate (Fig. 2*H*). However, HRP had a very small effect on the total oxidized products from Glc6 when using *Mt*CDH2, strongly suggesting these products were a direct result of PMO catalyzed O_2 activation (Fig. 2*H*).

O_2 Versus H_2O_2: Oxidation Analysis of *Mt*PMO9E and Glc6. Single and multiple turnover assays were employed to investigate the outcome of the *Mt*PMO9E reaction with either cosubstrate in the presence and absence of Glc6. In all reactions, the same amount of cosubstrate (75 μM) was consumed, enabling a direct comparison of each cosubstrate. The rapid consumption of H_2O_2 prevented measurement of its disappearance; however, based on the consumption of Glc6, all H_2O_2 was consumed over the course of the reaction (discussed below). O_2 consumption by *Mt*PMO9E was much slower, and hence it was recorded (*SI Appendix*, Fig. S6).

Global analysis of protein modification during turnover with either O_2 or H_2O_2 was assayed by MS (Fig. 3). Oxidation of the untreated sample was observed, indicating PMO oxidation occurred during the expression, purification, or processing of samples (Fig. 3*A*). The single turnover of O_2 in the absence and presence of Glc6 led to minimal, if any, oxidation of *Mt*PMO9E. When H_2O_2 was the substrate, the singly (+16 Da) and doubly (+32 Da) oxidized forms of the enzyme occurred at higher relative abundance than in the control (Fig. 3*A* and *SI Appendix*, Table S7). These oxidized forms of the enzyme were below detection limits when Glc6 was present in the assay.

Multiple turnovers of *Mt*PMO9E with O_2 in absence of Glc6 resulted in some oxidative modification of the enzyme, whereas in the presence of Glc6 no change in the overall extent of enzyme oxidation was observed (Fig. 3*B*). Conversely, multiple turnovers

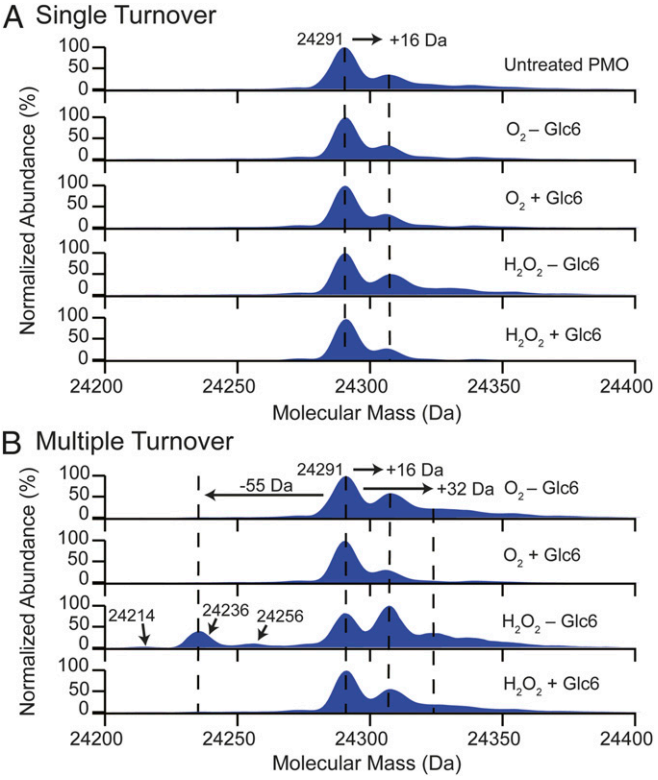

Fig. 3. Deconvoluted mass spectra of *Mt*PMO9E. (*A*) Single-turnover experiment with *Mt*PMO9E (75 μM) and Glc6 (0 or 2 mM) with either O_2 or H_2O_2 (75 μM). (*B*) Multiple-turnover experiment with *Mt*PMO9E (1 μM) and Glc6 (0 or 1 mM) and either O_2 or H_2O_2 (75 μM). All reactions were performed at a minimum in triplicate with similar resulting spectra. Values for normalized abundances can be found in *SI Appendix*, Tables S7 and S8.

with H_2O_2 in the absence of Glc6 led to extensive oxidation of *Mt*PMO9E (Fig. 3*B* and *SI Appendix*, Table S8). Previous work has shown oxidative modification of PMOs predominantly occurs on aromatic residues near the active site, and the Cu-coordinating His residues, which can lead to degradation of the His side chain (7). Consistent with these results, a modest fraction of the enzyme exhibited a decrease in molecular mass of 55 Da (Fig. 3*B*). In addition, activity of the H_2O_2-treated PMO decreased ~40%, compared with that of the untreated enzyme (*SI Appendix*, Fig. S7). It was clear Glc6 protected the enzyme from self-oxidation, as addition to identical reaction mixtures significantly decreased the extent of PMO oxidation (Fig. 3).

The oxidation products of Glc6 were also determined for each reaction using high-resolution MS. Each spectrum was analyzed for nonoxidized cellodextrin ions (GlcX; X = 2 ≤ degree of polymerization ≤ 6), 4-ketoaldose ions (GlcXox), and geminal diol ions (GlcXgem). All products were detected as ions with signal-to-noise ratios (S/N) above the cutoff value of 2. Based on the binding mode of Glc6 observed in the crystal structures of a fungal PMO (15), regioselective C4 oxidation of Glc6 is expected to generate only Glc2ox and Glc2gem products (Fig. 1).

Reactivity with O_2, independent of assay format, led to nearly exclusive formation of Glc2ox and Glc2gem ions (Table 1), as expected for regioselective hydroxylation of Glc6. Conversely, single-turnover experiments with H_2O_2 as the cosubstrate generated not only Glc2ox and Glc2gem ions but also Glc6ox ions. Multiple turnovers of *Mt*PMO9E with H_2O_2 produced a range of oxidized products (Table 1), suggesting the reaction with H_2O_2 leads to the formation of a nonselective oxidant. Although absolute product quantification was not possible due to the lack of standards for these compounds, it is noteworthy that the percent relative abundances of these products diminished with increasing

Table 1. Oxidation analysis of Glc6

Compound (M)	Chemical formula	Single turnover*		Multiple turnover†		Control reaction‡
		Percent relative abundance (H_2O_2)	Percent relative abundance (O_2)	Percent relative abundance (H_2O_2)	Percent relative abundance (O_2)	Percent relative abundance
Glc2	$C_{12}H_{22}O_{11}$	0.16 ± 0.03	0.15 ± 0.05	0.24 ± 0.03	0.18 ± 0.04	0.17 ± 0.06
Glc2ox	$C_{12}H_{20}O_{11}$	1.46 ± 0.55	0.92 ± 0.14	0.93 ± 0.10	1.32 ± 0.18	—
Glc2gem	$C_{12}H_{22}O_{12}$	4.70 ± 1.00	5.84 ± 0.77	3.97 ± 0.47	6.27 ± 0.79	—
Glc3	$C_{18}H_{32}O_{16}$	1.65 ± 0.27	1.45 ± 0.15	1.94 ± 0.43	0.71 ± 0.47	0.76 ± 0.28
Glc3ox	$C_{18}H_{30}O_{16}$	—	—	0.04 ± 0.01	—	—
Glc3gem	$C_{18}H_{32}O_{17}$	—	—	0.29 ± 0.02	0.08 ± 0.03	—
Glc4	$C_{24}H_{42}O_{21}$	4.37 ± 1.28	4.52 ± 0.39	5.43 ± 1.29	5.19 ± 1.51	2.34 ± 0.97
Glc4ox	$C_{24}H_{40}O_{21}$	—	—	0.07 ± 0.01	—	—
Glc4gem	$C_{24}H_{42}O_{22}$	—	—	0.08 ± 0.01	—	—
Glc5	$C_{30}H_{52}O_{26}$	7.28 ± 1.22	7.12 ± 1.08	7.29 ± 1.22	6.22 ± 1.14	3.87 ± 1.90
Glc6	$C_{36}H_{62}O_{31}$	80.27 ± 1.06	80.00 ± 0.88	79.26 ± 1.06	80.03 ± 1.12	92.86 ± 2.11
Glc6ox§,¶	$C_{36}H_{60}O_{31}$	0.11 ± 0.04	—	0.35 ± 0.10	—	—
Glc6_2ox§	$C_{36}H_{58}O_{31}$	—	—	0.11 ± 0.04	—	—

Percent relative abundance for each reaction was determined based on the sum of the absolute abundances of the $[M + H]^+$ and $[M + Na]^+$ adducts for all ions listed. Ions with no relative abundance value were below the limit of detection, defined as S/N <2. Error represents one SD of the mean.

*Assays contained *Mt*PMO9E (75 μM), ascorbate (2 mM), Glc6 (2 mM), and either O_2 or H_2O_2 (75 μM) in 50 mM MES and 50 mM MOPS, I = 100 mM, pH 6.5 ($n = 3$).

†Assays contained *Mt*PMO9E (1 μM), ascorbate (2 mM), Glc6 (1 mM), and either O_2 or H_2O_2 (75 μM) in 50 mM MES and 50 mM MOPS, I = 100 mM, pH 6.5 ($n = 3$).

‡Reaction contained ascorbate (2 mM), Glc6 (1 mM), and H_2O_2 (100 μM) in 50 mM MES and 50 mM MOPS, I = 100 mM, pH 6.5 and was incubated for 10 min. The same product profile was observed when H_2O_2 was replaced with O_2.

§See *SI Appendix*, Fig. S8 for potential corresponding chemical structures.

¶See *SI Appendix*, Fig. S9 for annotated MS/MS spectrum.

distance from the Cu active site. The observation of Glc6ox and Glc6_2ox ions indicates that oxidation is occurring at sites on the polysaccharide other than the C4 position as the glycosidic bond was not cleaved (*SI Appendix*, Fig. S8). These oxidized Glc6 species were not detected in control reactions and thus are not a result of nonenzymatic solution chemistry. The Glc6ox ion was further analyzed by tandem MS (MS/MS) to identify the site of oxidation. The precise location of the oxidation could not be unambiguously determined due to the low precursor ion abundance of this species compared with that of the substrate and the similarity of its mass (m/z = 989.31) to the substrate ion (m/z = 991.33). Nonetheless, the MS/MS spectrum is consistent with oxidation occurring on the third glucose monosaccharide residue from the reducing end of Glc6 at a position other than the C1 or C4 position (*SI Appendix*, Fig. S9).

Kinetics of H_2O_2 Reactivity. A significant decrease in the total amount of oxidized products from the insoluble substrates was observed with the addition of HRP, indicating that the majority of the products are a result of *Mt*PMO9E reacting with in situ-generated H_2O_2 (Fig. 1*A*). Given this result, we attempted to determine the steady-state kinetic parameters of cellodextrin oxidation using H_2O_2 as the cosubstrate. As homogenous solutions are needed for reliable steady-state kinetic data, Glc6 was the only suitable polysaccharide substrate for these assays.

*Mt*PMO9E oxidation of Glc6 by H_2O_2 required the addition of ascorbic acid. Unfortunately, in the presence of ascorbic acid initial rates corresponding to <15% consumption of the limiting reactant were too fast to be measured, even at relatively low H_2O_2 concentrations (12.5–100 μM) (*SI Appendix*, Fig. S10). However, observed rates corresponding to the consumption of >50% of H_2O_2 added could be determined (*SI Appendix*, Table S9). The observed rates (285–916 min^{-1}) indicated the PMO reacted faster with H_2O_2 than with O_2 (discussed below). Rate measurements for higher H_2O_2 concentrations (i.e., >100 μM) were not possible as the H_2O_2 was completely consumed before time points could be collected.

Steady-State Kinetics of the Oxygenase Reaction. Steady-state assays with Glc6 as the varied substrate were performed at a fixed O_2 concentration (206 μM) to probe the steps involved in the oxidation of the polysaccharide substrate. These assays were performed in the presence and absence of HRP to test if the in situ-generated H_2O_2 influenced the initial rates involved in the oxidation of Glc6 when O_2 was the cosubstrate (Fig. 4*A*). The kinetic parameter $k_{cat}/K_{m(Glc6)}$ encompasses initial rates with subsaturating Glc6 concentrations, steps where H_2O_2 reactivity would be most likely to influence activity. A threefold decrease in the apparent $k_{cat}/K_{m(Glc6)}$ [$k_{cat}/K_{m(O_2)} = 0.30 \pm 0.05$] was observed when HRP was present in the assay [$k_{cat}/K_{m(O_2)} = 0.11 \pm 0.02$] (*SI Appendix*, Table S10). This result is consistent with competing H_2O_2-mediated turnover. There was no significant difference between the apparent k_{cat} values determined in the presence (10.8 ± 0.6 min^{-1}) or absence (10.1 ± 0.2 min^{-1}) of HRP, strongly suggesting that H_2O_2, if generated, did not influence the oxygenase reaction when the PMO was saturated with Glc6.

Assays with varied O_2 used a Clark-type oxygen electrode to monitor O_2 consumption in the presence and absence of Glc6, probing the kinetics of O_2 reactivity for the coupled and uncoupled reaction, respectively. To ensure the *Mt*PMO9E was fully saturated with Glc6, a coupled assay detecting the formation of H_2O_2 was employed (Fig. 1*A*). The initial rate data with O_2 indicated that *Mt*PMO9E activity was dependent on O_2 concentration (Fig. 4*B*). A small decrease in the k_{cat} as well as the $K_{m(O_2)}$ was observed when the PMO was saturated with Glc6 [coupled reaction, k_{cat} = 17 ± 2 min^{-1}, $K_{m(O_2)}$ = 230 ± 31] compared with when Glc6 was absent [uncoupled reaction, k_{cat} = 26 ± 2 min^{-1}, $K_{m(O_2)}$ = 365 ± 45] (Fig. 4*B* and *SI Appendix*, Table S11). The $K_{m(O_2)}$ correlates closely with the concentration of dissolved oxygen under ambient conditions, consistent with PMO function in an extracellular environment. The $k_{cat}/K_{m(O_2)}$ values [$k_{cat}/K_{m(O_2)} = 0.074 \pm 0.014$] were independent of Glc6, indicating that the free enzyme and PMO/Glc6 complex react with O_2 at the same rate, regardless of whether O_2 reduction results in Glc6 hydroxylation.

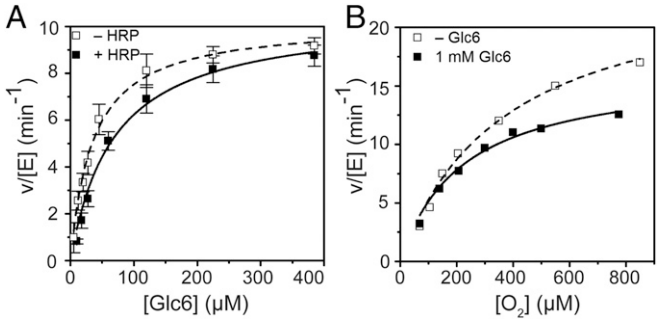

Fig. 4. Steady-state kinetics of the oxygenase reaction. (*A*) Varied Glc6 in the presence (■, solid line) or absence (□, dashed line) of HRP (1.3 μM) (n = 3). (*B*) Varied O_2, in the absence (□, dashed line) or presence (■, solid line) of 1 mM Glc6 (n = 3). See text and *SI Appendix*, Tables S10 and S11 for kinetic parameters.

Cellulose Degradation by *Neurospora crassa* Secretome. Although it is well known that PMOs work synergistically with other secreted cellulases to degrade biomass (23), the extracellular formation of H_2O_2 by oxidoreductases and oxidases could enhance PMO activity and overall cellulose degradation. To study the influence of H_2O_2 on the ability of the *N. crassa* secretome to degrade Avicel, HRP was added to degradation assays using the secretome from *N. crassa*. Based on proteomic analysis of this secretome (24, 25), HRP concentrations were selected to mirror similar HRP-to-PMO ratios used with purified proteins. The pink color of the reaction supernatant, resulting from the oxidation of the Amplex Red, indicated H_2O_2 was produced over the course of the reaction. However, over this range of HRP concentrations, there was no significant effect on the overall production of glucose (Fig. 5), suggesting H_2O_2 probably does not serve as a cosubstrate for PMOs in the secretome.

Discussion

Cu-mediated O-atom insertion reactions have been intensely studied with Cu-metalloenzymes and biomimetic inorganic complexes (26–30). These complementary approaches have provided rationale and insight into the molecular mechanisms of Cu-dependent hydroxylations. Biologically relevant mechanisms have primarily focused on O_2 as the cosubstrate. The catalytic cycle begins with reduction of Cu(II) followed by O_2 binding to the Cu(I) site, forming a Cu(II)–superoxide complex. From this common point opinions diverge with respect to the identity of the hydrogen atom abstraction (HAA) species and the cleavage of the O–O bond. The primary differences result from the timing of the delivery of protons and electrons to the Cu/O_2 complex. However, H_2O_2 has been shown to react with biomimetic Cu(I) complexes to oxidize substrates through Fenton-like chemistry, where homolytic cleavage of the O–O bond generates powerful and nonselective hydroxyl radicals (31–33).

Evidence has pointed to O_2 as the cosubstrate for the mononuclear Cu center in PMOs (16, 17), but a recent report concluded that H_2O_2 is the cosubstrate (7). Some of the results presented here agree with this report (Fig. 2 *B* and *C*) but differ in interpretation of the data based on additional experiments with higher concentrations of insoluble substrates (Fig. 2 *E* and *F*) and, more importantly, experimental data using a soluble substrate (Fig. 2 *D* and *G*). PMOs are capable of utilizing either H_2O_2 (peroxygenase activity) or O_2 (oxygenase activity) (Fig. 1*A*). Reaction conditions, more specifically the polysaccharide concentration, have a significant impact on the cosubstrate utilized (Fig. 2). The binding of polysaccharides by PMOs is relatively weak (34), such that a large fraction of enzyme is unbound at low substrate concentrations, generating the more reactive cosubstrate H_2O_2 that can outcompete O_2 (Fig. 1*A*, pathway b). However, polysaccharide saturation can be achieved with a soluble cello-oligosaccharide (Glc6) and these experiments demonstrate that oxygenase chemistry is the exclusive pathway of hydroxylation (Fig. 1*A*, pathway a). Active-site occupancy is crucial for oxygenase activity, but this is difficult to achieve with insoluble polymeric substrates. The results here show that oxygenase activity increases with increasing concentrations of the insoluble substrates and is always favored with Glc6. In addition, the precise timing of electron transfer governs the formation of the active-site oxidant and limits the uncoupled reaction. Indeed, when CDH was used as the sole electron donor for the PMO reaction with Glc6, the products were almost exclusively a result of oxygenase activity (Fig. 2*G*). This is also apparent in light-driven reduction of PMOs, where the addition of reactive oxygen species scavengers had no effect on PASC oxidation (35).

The results here show that PMOs can function with either H_2O_2 or O_2; however, the reactions are mechanistically distinct as different products are observed. The oxygenase mechanism carries out regioselective oxidation leading to cleavage of the glycosidic bond (only Glc2ox products) without oxidative damage to the enzyme. This is consistent with the evolution of an enzyme that would control the reactivity of the oxidant and limit turnover-dependent inactivation Perhaps the low $k_{cat}/K_{m(O_2)}$ values combined with the high $K_{m(O_2)}$ values serve as a protective kinetic feature of PMOs in an effort to minimize uncoupled turnover. In addition, the PMO second coordination sphere residues are positioned to stabilize a cupric superoxide species (23, 36, 37). While extensive experimental work continually points to a cupric superoxide species for HAA by Cu enzymes (12, 28, 38), computational work has favored Cu-oxyl–based mechanisms for PMOs (39, 40). Conversely, the peroxygenase mechanism appears to involve hydroxyl radical chemistry resulting from Fenton-like chemisty with H_2O_2 and Cu(I). In the absence of a polysaccharide substrate, this Fenton-like chemistry leads to protein modification and loss of activity; these observations are consistent with indiscriminate reactivity resulting from the generation of hydroxyl radicals. It is known that polysaccharides are suitable hydroxyl radical scavengers (41); this is apparent from the protective role of Glc6 against enzyme modification and the relative lack of regioselective oxidation observed with H_2O_2. The close proximity of the glycosidic bond between the second and third glycosyl unit favors the C4 position for hydroxyl radical chemistry, but other bonds of the polysaccharide are also oxidized (Table 1), as expected with hydroxyl radical chemistry. Indeed, a recent computational study indicated hydroxyl radicals are generated in the peroxygenase reaction (42).

The ability of a PMO to function as either a peroxygenase or oxygenase is intriguing. Based on X-ray structural data with another PMO, the polysaccharide substrate binds with the C4 positioned over the Cu active site (Fig. 1*B*) (15), such that the formation of a reactive oxidant, regardless of cosubstrate identity,

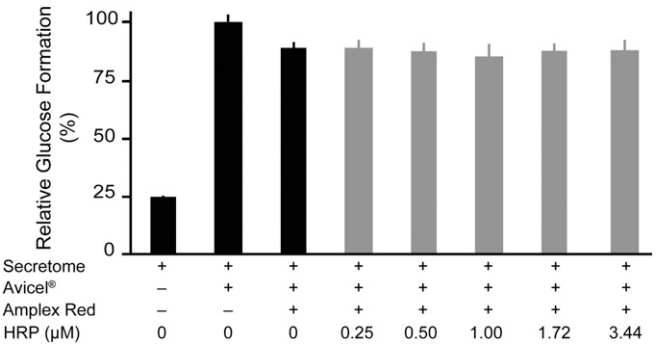

Fig. 5. Degradation of Avicel using cultured secretome. Reactions were incubated at 40 °C for 1 h with constant shaking (850 rpm). The resulting supernatant was incubated with glucosidase before the determination of total glucose using a glucose oxidase/peroxidase coupled assay (n = 4). Error bars represent one SD of the mean.

BIOCHEMISTRY

is competent for HAA. However, the question arises as to which cosubstrate is used in nature. It is tempting to favor the peroxygenase reactivity, especially considering H_2O_2-generating oxidases are secreted with PMOs (43). However, degradation of Avicel by cultured *N. crassa* secretome was not influenced by the addition of exogenous HRP (Fig. 5). The formation of H_2O_2 by these enzymes appears to be tightly regulated and likely intended for extracellular peroxidases, not PMOs. Thus, the available concentration of "free" H_2O_2 may not be able to compete with the abundance of O_2 typically found in extracellular environments. Although the monooxygenase reaction is significantly slower than the peroxygenase reaction, regioselective hydroxylation is achieved and, more importantly, there is minimal oxidative damage to the PMO, regardless if substrate is present. This allows the PMO to function without inactivation. The peroxygenase reaction is less regioselective and results in extensive detrimental oxidative damage to the enzyme, begging the question if H_2O_2 is an intended physiological cosubstrate for PMOs.

Overall, PMOs catalyze both peroxygenase and oxygenase reactions to oxidize insoluble and soluble polysaccharides. These results demonstrate that O_2 is a cosubstrate for PMO reactions in the hydroxylation of polysaccharides. With the reduced Cu(I) form of the enzyme, H_2O_2 is a much faster cosubstrate but suffers from the outcomes noted above. Our data provide a basis for understanding the kinetics involved in O_2 activation and Glc6 oxidation. Additional efforts will be necessary to fully understand the reactivity of PMOs with O_2 and decipher the intricate molecular details of the O_2-catalyzed reaction.

Materials and Methods

Detailed materials and methods are provided in *SI Appendix, Experimental Procedures*. All assays used Cu-reconstituted *Mt*PMO9E. Reactions were monitored using either high-performance anion-exchange chromatography (HPAEC) or a Clark-type electrode. Products were analyzed using HPAEC and LC-MS. Intact MS was performed using a Synapt G2-Si.

ACKNOWLEDGMENTS. We thank Stefan Kapczynski for assistance in the preparation of *Mt*PMO9E, Elise Span for preparation of *Mt*CDH2, Judith Klinman for use of the Hansatech Oxygraph instrument, Cheri Ackerman for the inductively coupled plasma MS analysis, and the members of the M.A.M. laboratory for critical reading of the manuscript. This work was supported by NSF Grant 1565770. The QB3/Chemistry Mass Spectrometry Facility at the University of California, Berkeley receives support from National Institutes of Health Grant 1S10OD020062-01.

1. Klinman JP (2007) How do enzymes activate oxygen without inactivating themselves? *Acc Chem Res* 40:325–333.
2. Busk PK, Lange L (2015) Classification of fungal and bacterial lytic polysaccharide monooxygenases. *BMC Genomics* 16:368.
3. Hemsworth GR, Johnston EM, Davies GJ, Walton PH (2015) Lytic polysaccharide monooxygenases in biomass conversion. *Trends Biotechnol* 33:747–761.
4. Corrêa TLR, dos Santos LV, Pereira GAG (2016) AA9 and AA10: From enigmatic to essential enzymes. *Appl Microbiol Biotechnol* 100:9–16.
5. Agostoni M, Hangasky JA, Marletta MA (2017) Physiological and molecular understanding of bacterial polysaccharide monooxygenases. *Microbiol Mol Biol Rev* 81: e00015-17.
6. Johansen KS (2016) Lytic polysaccharide monooxygenases: The microbial power tool for lignocellulose degradation. *Trends Plant Sci* 21:926–936.
7. Bissaro B, et al. (2017) Oxidative cleavage of polysaccharides by monocopper enzymes depends on H_2O_2. *Nat Chem Biol* 13:1123–1128.
8. Wang X, Peter S, Kinne M, Hofrichter M, Groves JT (2012) Detection and kinetic characterization of a highly reactive heme-thiolate peroxygenase compound I. *J Am Chem Soc* 134:12897–12900.
9. Peter S, et al. (2011) Selective hydroxylation of alkanes by an extracellular fungal peroxygenase. *FEBS J* 278:3667–3675.
10. Kjaergaard CH, et al. (2014) Spectroscopic and computational insight into the activation of O_2 by the mononuclear Cu center in polysaccharide monooxygenases. *Proc Natl Acad Sci USA* 111:8797–8802.
11. Kittl R, Kracher D, Burgstaller D, Haltrich D, Ludwig R (2012) Production of four Neurospora crassa lytic polysaccharide monooxygenases in *Pichia pastoris* monitored by a fluorimetric assay. *Biotechnol Biofuels* 5:79–92.
12. Klinman JP (2006) The copper-enzyme family of dopamine β-monooxygenase and peptidylglycine α-hydroxylating monooxygenase: Resolving the chemical pathway for substrate hydroxylation. *J Biol Chem* 281:3013–3016.
13. Bennati-Granier C, et al. (2015) Substrate specificity and regioselectivity of fungal AA9 lytic polysaccharide monooxygenases secreted by *Podospora anserina*. *Biotechnol Biofuels* 8:90.
14. Isaksen T, et al. (2014) A C4-oxidizing lytic polysaccharide monooxygenase cleaving both cellulose and cello-oligosaccharides. *J Biol Chem* 289:2632–2642.
15. Frandsen KEH, et al. (2016) The molecular basis of polysaccharide cleavage by lytic polysaccharide monooxygenases. *Nat Chem Biol* 12:298–303.
16. Vaaje-Kolstad G, et al. (2010) An oxidative enzyme boosting the enzymatic conversion of recalcitrant polysaccharides. *Science* 330:219–222.
17. Beeson WT, Phillips CM, Cate JHD, Marletta MA (2012) Oxidative cleavage of cellulose by fungal copper-dependent polysaccharide monooxygenases. *J Am Chem Soc* 134: 890–892.
18. Payne CM, et al. (2015) Fungal cellulases. *Chem Rev* 115:1308–1448.
19. Zhang YHP, Lynd LR (2004) Toward an aggregated understanding of enzymatic hydrolysis of cellulose: Noncomplexed cellulase systems. *Biotechnol Bioeng* 88:797–824.
20. Phillips CM, Beeson WT, Cate JH, Marletta MA (2011) Cellobiose dehydrogenase and a copper-dependent polysaccharide monooxygenase potentiate cellulose degradation by Neurospora crassa. *ACS Chem Biol* 6:1399–1406.
21. Langston JA, et al. (2011) Oxidoreductive cellulose depolymerization by the enzymes cellobiose dehydrogenase and glycoside hydrolase 61. *Appl Environ Microbiol* 77: 7007–7015.
22. Tan TC, et al. (2015) Structural basis for cellobiose dehydrogenase action during oxidative cellulose degradation. *Nat Commun* 6:7542.
23. Harris PV, et al. (2010) Stimulation of lignocellulosic biomass hydrolysis by proteins of glycoside hydrolase family 61: Structure and function of a large, enigmatic family. *Biochemistry* 49:3305–3316.
24. Phillips CM, Iavarone AT, Marletta MA (2011) Quantitative proteomic approach for cellulose degradation by *Neurospora crassa*. *J Proteome Res* 10:4177–4185.
25. Tian C, et al. (2009) Systems analysis of plant cell wall degradation by the model filamentous fungus *Neurospora crassa*. *Proc Natl Acad Sci USA* 106:22157–22162.
26. Quist DA, Diaz DE, Liu JJ, Karlin KD (2017) Activation of dioxygen by copper metalloproteins and insights from model complexes. *J Biol Inorg Chem* 22:253–288.
27. Liu JJ, Diaz DE, Quist DA, Karlin KD (2016) Copper(I)-dioxygen adducts and copper enzyme mechanisms. *Isr J Chem* 56:9–10.
28. Cowley RE, Tian L, Solomon EI (2016) Mechanism of O_2 activation and substrate hydroxylation in noncoupled binuclear copper monooxygenases. *Proc Natl Acad Sci USA* 113:12035–12040.
29. Neisen BD, Gagnon NL, Dhar D, Spaeth AD, Tolman WB (2017) Formally copper(III)-alkylperoxo complexes as models of possible intermediates in monooxygenase enzymes. *J Am Chem Soc* 139:10220–10223.
30. Itoh S (2015) Developing mononuclear copper-active-oxygen complexes relevant to reactive intermediates of biological oxidation reactions. *Acc Chem Res* 48:2066–2074.
31. Kim S, et al. (2015) Amine oxidative N-dealkylation via cupric hydroperoxide Cu-OOH homolytic cleavage followed by site-specific fenton chemistry. *J Am Chem Soc* 137: 2867–2874.
32. Trammell R, et al. (2017) Decoding the mechanism of intramolecular Cu-directed hydroxylation of sp^3C-H bonds. *J Org Chem* 82:7887–7904.
33. Garcia-Bosch I, Siegler MA (2016) Copper-catalyzed oxidation of alkanes with H_2O_2 under a Fenton-like Regime. *Angew Chem Int Ed Engl* 55:12873–12876.
34. Courtade G, et al. (2016) Interactions of a fungal lytic polysaccharide monooxygenase with β-glucan substrates and cellobiose dehydrogenase. *Proc Natl Acad Sci USA* 113: 5922–5927.
35. Möllers KB, et al. (2017) On the formation and role of reactive oxygen species in light-driven LPMO oxidation of phosphoric acid swollen cellulose. *Carbohydr Res* 448: 182–186.
36. Span EA, Suess DLM, Deller MC, Britt RD, Marletta MA (2017) The role of the secondary coordination sphere in a fungal polysaccharide monooxygenase. *ACS Chem Biol* 12:1095–1103.
37. Hedegård ED, Ryde U (2017) Multiscale modelling of lytic polysaccharide monooxygenases. *ACS Omega* 2:536–545.
38. Kim S, et al. (2015) A N3S(thioether)-ligated Cu(II)-superoxo with enhanced reactivity. *J Am Chem Soc* 137:2796–2799.
39. Kim S, Ståhlberg J, Sandgren M, Paton RS, Beckham GT (2014) Quantum mechanical calculations suggest that lytic polysaccharide monooxygenases use a copper-oxyl, oxygen-rebound mechanism. *Proc Natl Acad Sci USA* 111:149–154.
40. Bertini L, et al. (2018) Catalytic mechanism of fungal lytic polysaccharide monooxygenases investigated by First-Principles calculations. *Inorg Chem* 57:86–97.
41. Vreeburg RA, Airianah OB, Fry SC (2014) Fingerprinting of hydroxyl radical-attacked polysaccharides by N-isopropyl-2-aminoacridone labelling. *Biochem J* 463:225–237.
42. Wang B, et al. (2018) QM/MM studies into the H_2O_2-dependent activity of lytic polysaccharide monooxygenases: Evidence for the formation of a caged hydroxyl radical intermediate. *ACS Catal* 8:1346–1351.
43. Kracher D, et al. (2016) Extracellular electron transfer systems fuel cellulose oxidative degradation. *Science* 352:1098–1101.